Static seals for hydrogen at high pressure

Agim Gashi, Lucian Pasieka

Simulating and evaluating the sealing capability of gasket material with the help of a Finite Element Analysis method is still a challenge when it is applied for gaseous hydrogen system where high pressure and low temperature are present. In our paper we show the preparation and execution of a FEA of a static O-ring seal which is designed for gaseous hydrogen application. The aim was to perform a simulation to verify the reliability capability of a seal already in service under a temperature range from -40°C up to T = + 85°C and a system pressure of up to p = 1000 bar. Material investigations were carried out to establish the basis of a suitable material model. As to evaluate the quality of the sealing we choose to use the contact pressure between the O-ring and the surrounding surfaces.

1 Introduction

At first, we created a hyperelastic model of the material used in this study. To do this, we obtained an 2mm thick plate of the selected material from a standard manufacturer and cut-out tensile specimens. The specimens were used to performed uniaxial and biaxial tensile tests at room temperature. We then performed measurements to determine the bulk modulus of this EPDM material. In parallel, we commissioned a DMA analysis to obtain the complete temperature-time behaviour. With this data, we created a master curve that we could describe with Prony parameters and use as material data in ANSYS. With the previous work we created a complex thermovisco-elastic material model based on measured data. This new model has allowed us to perform FEA which are more realistic for hydrogen gas under high pressure.

Due to the low temperature requirement, material with glass transition temperature T_g below = -50 °C and a compatibility with general resistance to gaseous hydrogen, an ethylene propylene diene monomer rubber (EPDM) with a hardness of 90 Shore A was chosen for this application.

1.1 Hyper elastic Material model

Using the measurement data from uniaxial and biaxial tensile tests, a Mooney-Rivlin model with two parameters was chosen as a suitable representation, see Eq. 1 and 2 [4] and Fig 1.

$$\sigma_{un} = 2c_{10}\left(\lambda - \frac{1}{\lambda^2}\right) + 2c_{01}\left(1 - \frac{1}{\lambda^3}\right) \tag{1}$$

$$\sigma_{bi} = 2c_{10}\left(\lambda - \frac{1}{\lambda^5}\right) + 2c_{01}\left(\lambda^3 - \frac{1}{\lambda^3}\right) \tag{2}$$

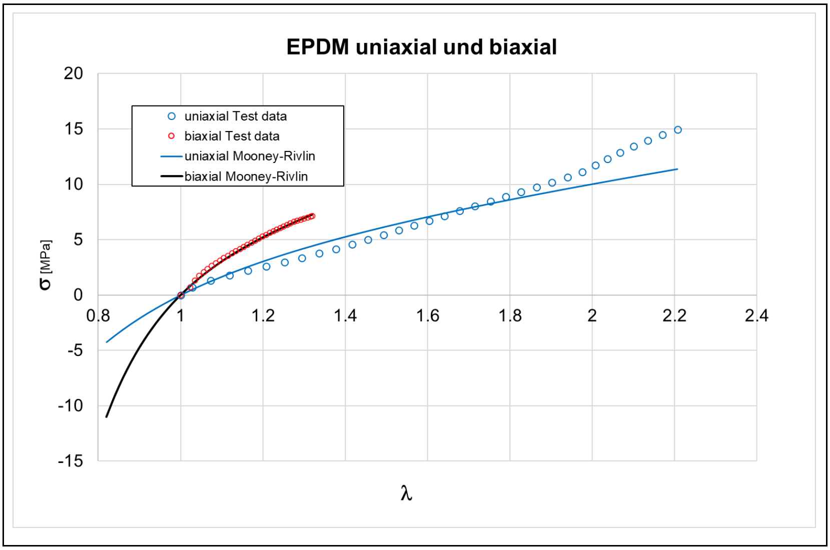

Figure 1: Mooney Rivlin uniaxial and biaxial

1.2 Bulk Modulus

Like most of the available material models we also created our model on the assumption of incompressibility. The questions which should be clarified is by how much percent, in the application, will the seal be compressed at 1000 bar? For this purpose, a small test device was used, with which the compression modulus can be determined up to 1000 bar [3]. For this study, we have only carried out these measurements at room temperature (RT), Figure 2.

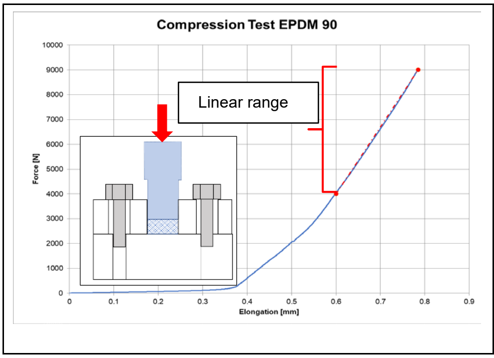

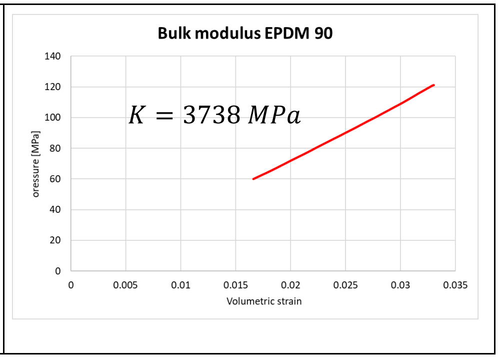

Figure 2: compression Test *Figure 3: Bulk modulus – linear range*

With the help of this data, the compression modulus K was determined, see Figure 3. At a pressure of 1000 bar, the material is compressed by a maximum of 3.3%. Due to the negligeable significance of such a small deformation was not included in the FEA in order to eliminate convergence problems.

1.3 Master curve for EPDM 90

The starting point for the master curve is a Dynamic Mechanical Analysis (DMA), see Fig. 4.

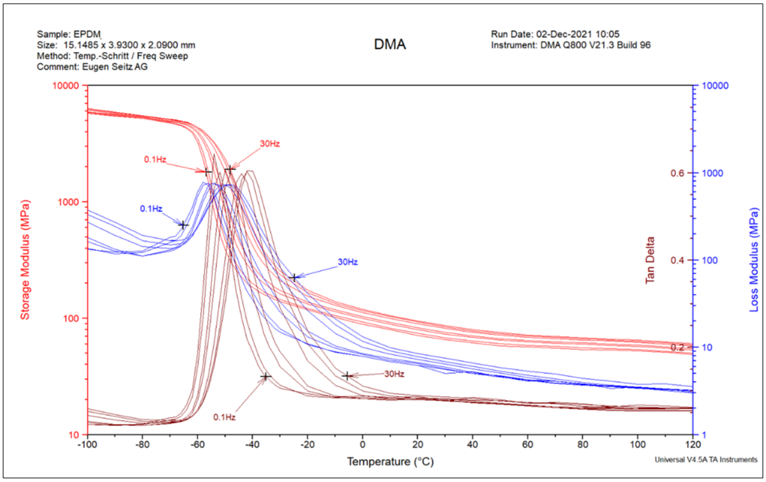

Figure 4: Dynamic Mechanical Analysis (DMA) EPDM 90

With the help of ViscoShift [1], it is very easy to create a master curve from the storage module. The following figures show the properties E', E'', E^* and $tan\delta$, see Figure 5… 8.

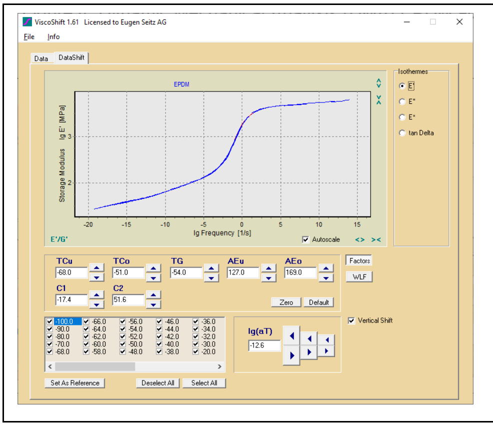

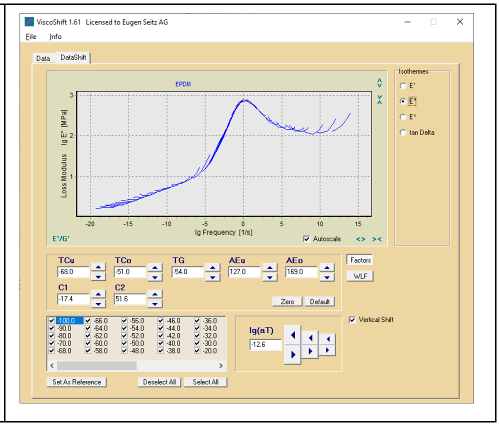

Figure 5: Storage Modulus E' *Figure 6: Loss Modulus E''*

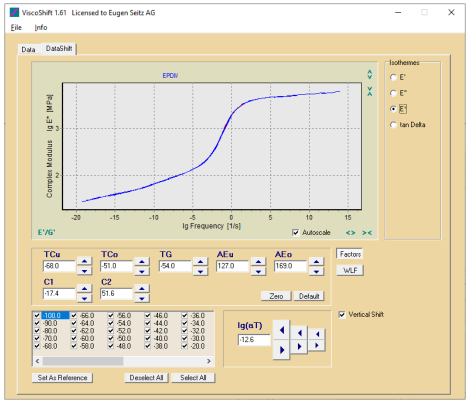

Figure 7: Complex Modulus E^*

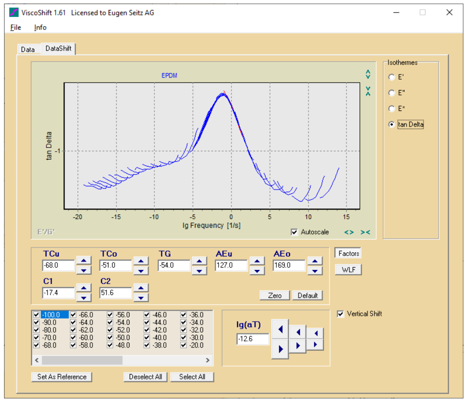

Figure 8: $\tan\delta$

In the same tool, it is also possible to obtain a visualization of the shift function, see figure 9, with the associated parameters, see Figure 10. Pairs of values, shown here as points, can be saved. They contain the shift information, by what amount the master curve must be shifted (log a_T) to obtain the data for a different temperature.

The equations for the complete calculation of the shift function are not listed here, but reference is made to the literature [1].

With the help of ViscoData, the Prony parameters of the master curve can be retrieved from the storage module using a special regression algorithm, see figure 11 and 12.

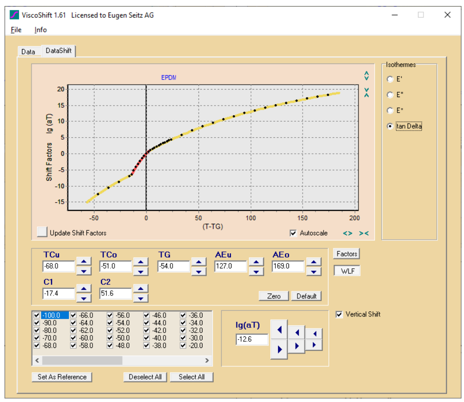

T_a	-54	°C
c_1	17.4	-
c_2	51.6	K
T_g	-54	°C
T_{cu}	-68	°C
T_{co}	-51	°C
A_{EU}	127	kJ/mol
A_{EO}	169	kJ/mol
R	0.008314	kJ/mol K
M	0.434	Umrechnung von ln in lg (= log e)

For the calculation of the shift function see [1], page 16.

Figure 9: Shift Function

Figure 10: Parameter Shift Function

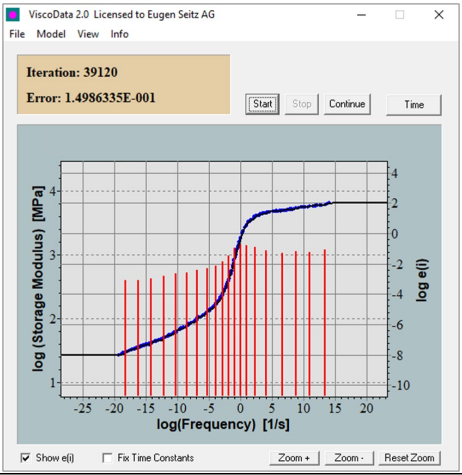

N	e_i	τ_i
1	8.19E-02	5.48E-15
2	5.60E-02	1.77E-12
3	6.56E-02	2.66E-10
4	5.17E-02	3.87E-08
5	7.49E-02	1.27E-05
6	1.32E-01	8.39E-04
7	1.69E-01	1.75E-02
8	1.82E-01	1.63E-01
9	1.06E-01	1.26E+00
10	3.69E-02	1.02E+01
11	1.50E-02	1.03E+02
12	7.55E-03	1.30E+03
13	5.09E-03	3.05E+04
14	3.72E-03	1.25E+06
15	2.59E-03	4.43E+07
16	2.42E-03	3.16E+09
17	1.50E-03	2.47E+11
18	1.04E-03	2.25E+13
19	8.78E-04	2.80E+15
20	8.71E-04	2.28E+17

$E_0 = 6350\ MPa$

$E_\infty = 27.3\ MPa$

Figure 11: Master curve *Figure 12: Prony parameter*

In this way, one obtains the master curve and a discrete relaxation spectrum, see figure 11, a basis for being able to describe further viscoelastic properties in a frequency-dependent manner. Starting from the generalised Maxwell model with 20 parallel Maxwell elements, which can be described with the help of Eq. (3).

$$E' = E_0 \left(1 - \sum_{i=1}^{20} \frac{e_i}{1+(\tau_i \cdot 2 \cdot \pi \cdot a_T \cdot f)^2}\right) \qquad (3)$$

With the shift factor a_T the master curve can be shifted to the desired temperature, see figure 13. What can also be seen in Eq. (3), is that the master curve of the storage modulus is created by the summation of relaxation times and strengths, having as starting point the largest value E_0. This explain why the hyperelastic material model must be scaled in ANSYS WB FEA to realize the coupling with the Prony parameters.

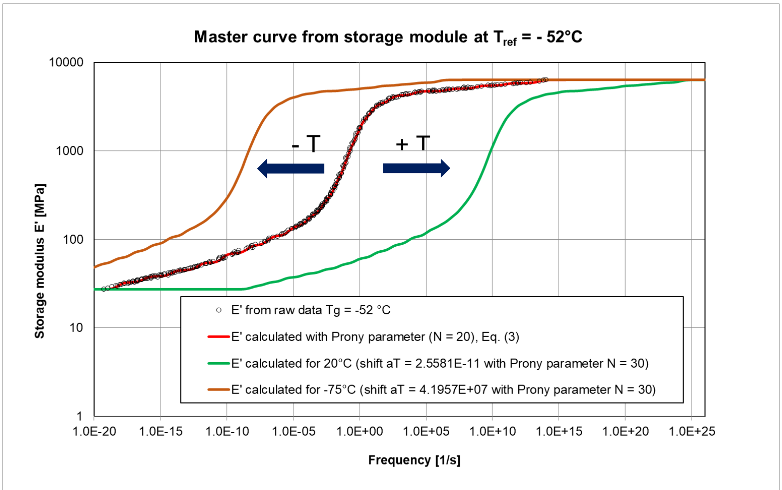

Figure 13: Master curve by different temperatures

1.4 Consideration of the shift of the glass transition at increased hydrostatic pressure

We refer to previously published investigations on the temperature-pressure shift ratio according to [2]. As seen in eq. (4), for the selected polymers, we use a shift according to Fillers and Tschoegl [3].

$$log\ a_P = C\ (p - p_0) \qquad \text{with} \qquad C \approx 0.025 \frac{K}{bar} \tag{4}$$

This means that for a pressure increase of 1000 bar a shift of + 25 K from the glass transition must be considered. In the FEA analysis this is considered with a temperature shift corresponding to the pressure, see section 2.2.

2 FEA implementation and results

With the material model described above, the following load sequences for the EPDM O-ring can be simulated in ANSYS (Workbench 2022 R1).

2.1 Load sequences

Table 1: Load sequences for FEA

Load step	parameters
1	The O-ring is expanded at T = 20°C
2	The O-ring is pressed into groove at T = 20°C
3	A system pressure of p = 1000 bar is applied via Fluid Pressure Macro at T = 20°C
4	The temperature is reduced from T = 20°C to T = -50°C at 1000 bar
5	The pressure is reduced from p = 1000 bar to p = 600 bar at T = -50°C
6	The temperature is increased from T = -50°C to T = 20°C keeping the pressure at 600 bar
7	One hour relaxation at T = 20°C and p = 600 bar

2.2 Comparison of system pressure and hydrostatic pressure

The following graph shows the difference between the system pressure and the hydrostatic pressure, see figure 14 and 15.

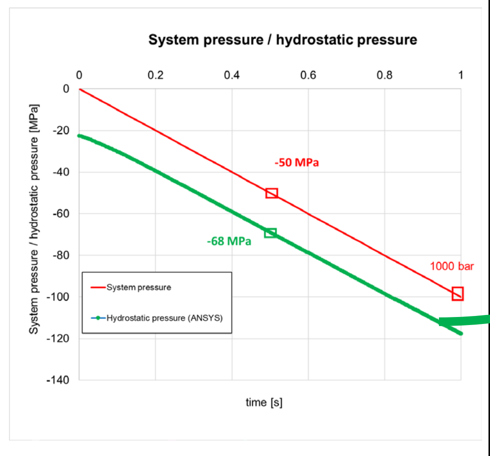

Figure 14: Comparison of average system pressure vs. hydrostatic pressure

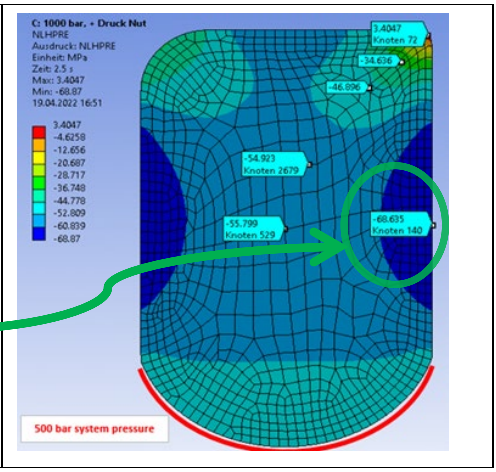

Figure 15: FEA hydrostatic pressure with system pressure of p = 500 bar

This shows that in large parts of the cross-section, the hydrostatic pressure is higher than the system pressure, up to 35% higher. Furthermore, the hydrostatic pressure near the gap of the O-ring is far below the system pressure. To consider a more accurate calculation of the actual displacement from the glass transition, an allocation of the material data per element would be necessary. For simplification, it is assumed that the system pressure is approximately equal to the hydrostatic pressure.

2.3 FEA model

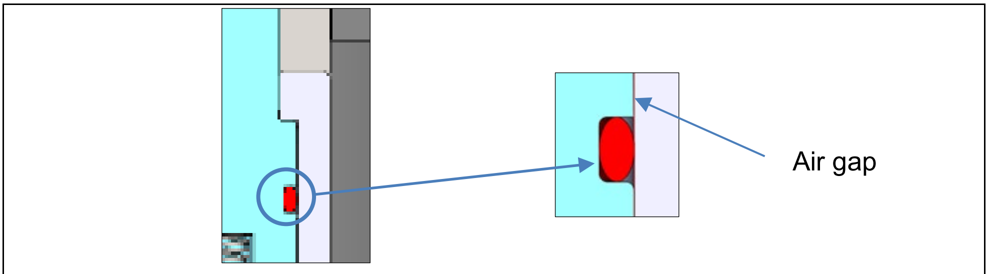

Figure 16: O-ring installation situation

The O-ring is installed between a shaft and an outer tube made of stainless steel. For the simulation, the air gap was set at 0.01 mm.

2.4 FEA according to the load steps (see section 2.1)

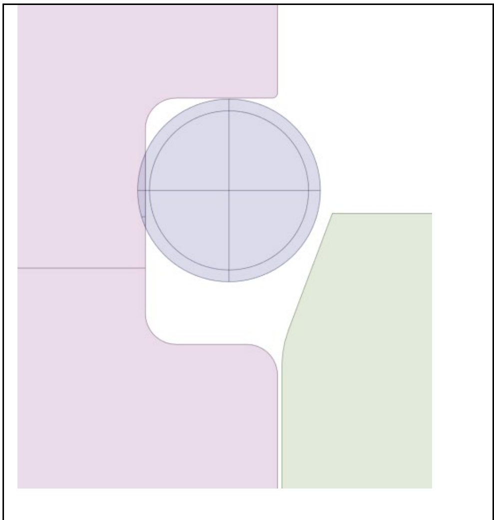

Figure 17: Axisymmetric 2D model with air gap of 0.01 mm

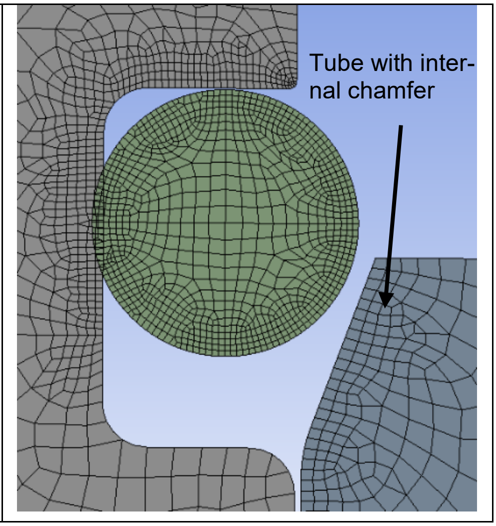

Figure 18: Before installation (unpressed)

In the **first load step**, the O-ring is expanded to be afterward pressed from the outside during the **second load case**. This is corresponding to the groove geometry in the installed state. In this case, a tube with an internal chamfer is pulled over the O-ring to obtain the desired compression. The installation situation is reached after load case 2.

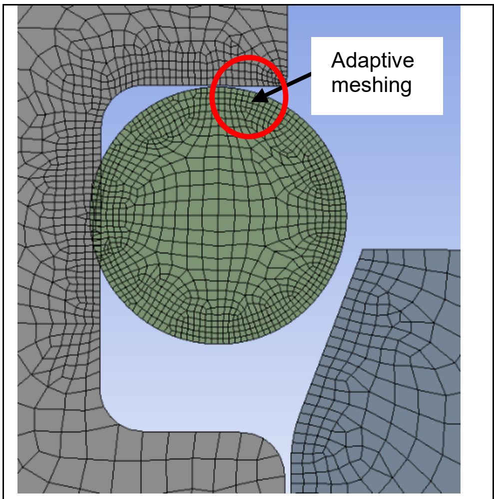

Figure 19: Adaptive meshing

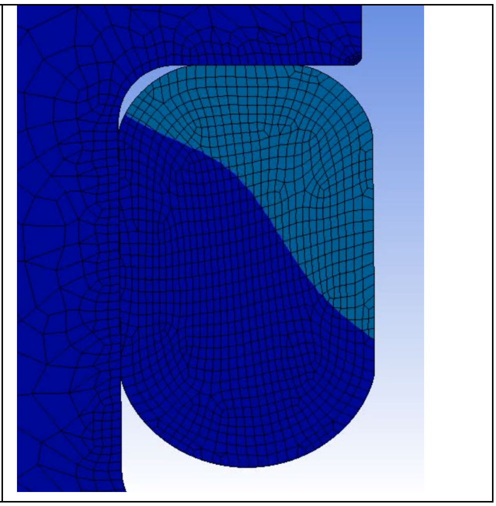

Figure 20: p = 0 bar system pressure (load step 2)

Figure 20 shows the O-ring in the installed condition after **load step 2**.

In **load step 3**, the system pressure of 1000 bar is applied via the Fluid Pressure macro (at T = 20°C), see figure 21 and 22. To obtain a better resolution for a possible gap extrusion in the air gap, the adaptive meshing of ANSYS is switched on. Depending on the settings, this performs one or more mesh refinement(s) during the calculation. Adaptive meshing avoids strong distortions of the elements, so that convergence problems are also avoided. Figure 22 shows the O-ring at a system pressure of 1000 bar (load step 3). A slight gap extrusion can be seen, which is not considered critical.

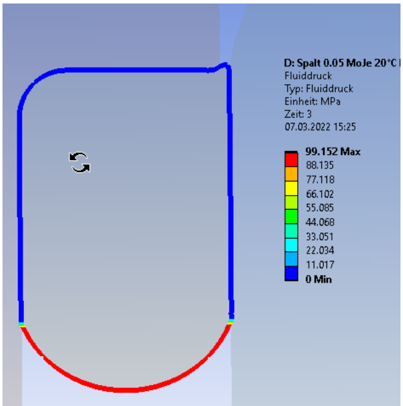

Figure 21: p = 1000 bar system pressure (after load step 3).

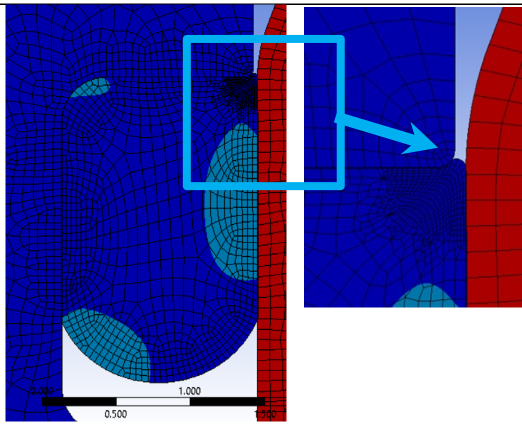

Figure 22: p = 1000 bar system pressure (after load step 3) low tendency to gap extrusion

The system pressure is applied accordingly to the Fluid Pressure macro and only onthe surfaces of the O-ring that are not in contact with the steel surface, Figure 21. After each iteration, the contact status is checked so that the system pressure can be applied to the corresponding surface. The system pressure on the O-ring thus corresponds as close as possible to the real conditions.

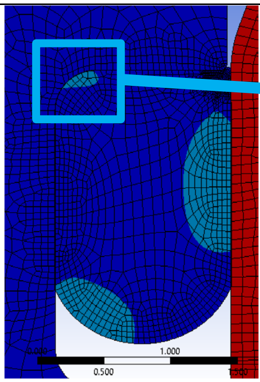

Figure 23: stress peaks in the groove

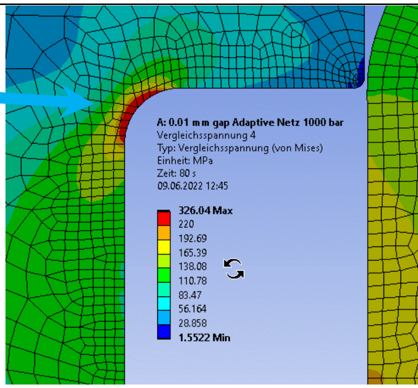

Figure 24: Mises stress in the groove

The maximum stresses (von Mises) in the groove are approximatively 320 MPa. This stress is not particularly critical for the material shaft used for the shaft.

To make a statement about the tightness quality, the contact pressure between the O-ring and the surrounding surfaces is evaluated. In the following figure, one can see that the pressure goes up to 121 MPa, which represents sufficient tightness against the system pressure of 1000 bar.

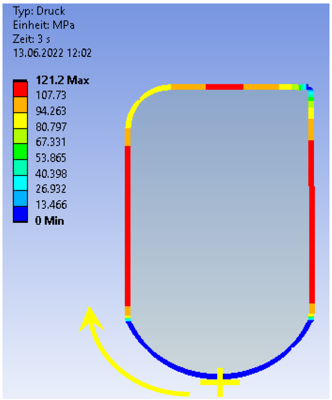

Figure 25: Contact pressure at system pressure 1000 bar

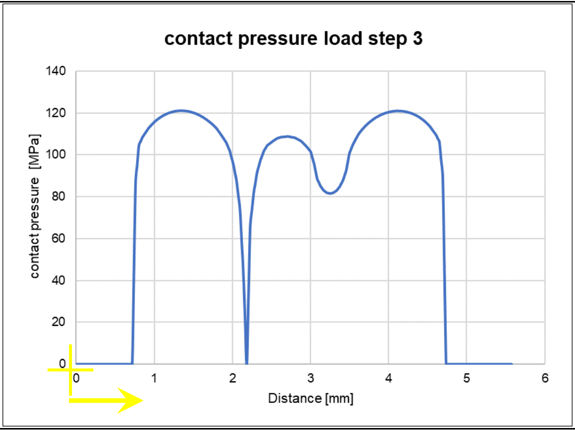

Figure 26: Contact pressure at the circumference of the seal at 1000 bar and 20°C

Figure 26 shows the course of the contact pressure around the circumference of the O-ring. The x-axis is the path around the circumference of the O-ring starting at bottom dead center (see Fig. 25 in yellow) in a clockwise direction. The y-axis is the contact pressure at the O-ring.

In **load step 4 (figure 27)**, the temperature is reduced from 20°C to -50°C at a constant pressure of 1000 bar. The following figure shows the contact pressure of the O-ring at -50°C. The contact pressure is not significantly affected by the "freezing" of the O-ring.

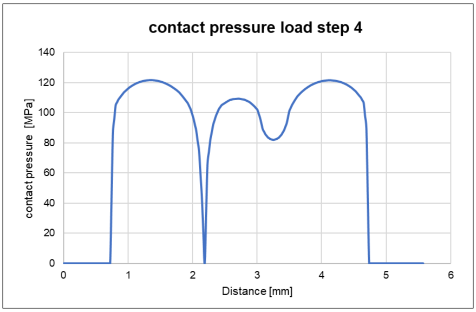

Figure 27: Contact pressure at p = 1000 bar and T = -50°C

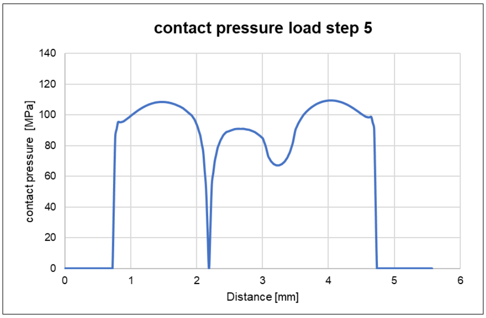

Figure 28: Contact pressure at p = 600 bar and T = -50°C.

In **load step 5 (figure 28),** the pressure is reduced from 1000 bar to 600 bar, keeping the temperature at -50°C. Despite the significant system pressure reduction, the contact pressure remains at a high level, just under 110 MPa, see figure 28.

In **load step 6**, the temperature is increased from -50°C to 20°C keeping the pressure constant at 600bar. The temperature increase leads to a significant contact pressure reduction. The O-ring "thaws" and is no longer in a glassy state. However, at 82 MPa, the sealing effect at 600 bar is sufficient to assure tightness.

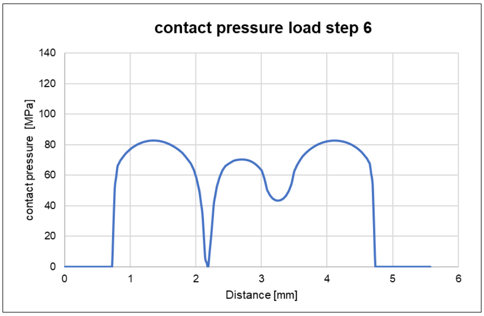

Figure 29: Contact pressure at 600 bar and 20°C

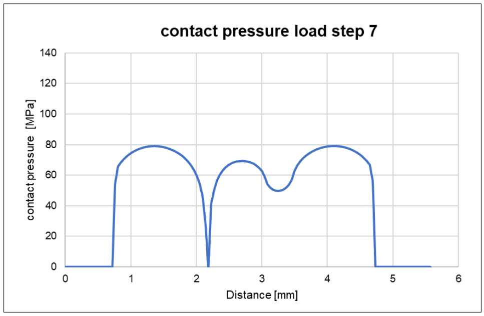

Figure 30: Contact pressure loss due to relaxation after one hour

In **load step 7**, the O-ring is relaxed at 600 bar and 20°C for one hour. The reduction of the sealing effect of the O-ring resulting from the relaxation is to be determined. This results in a reduction of the contact pressure of approx. 5.5% in one hour, see figure 31 and 9.4% for one day.

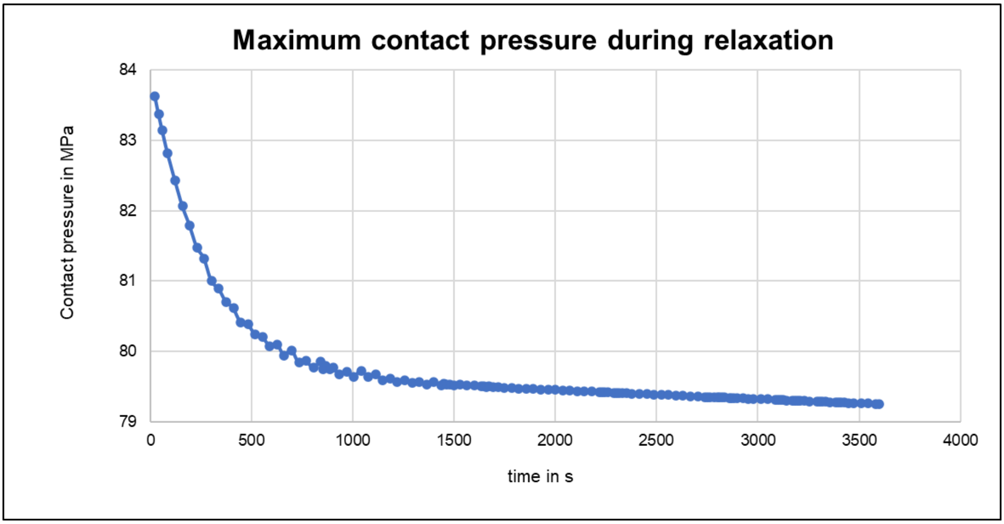

Figure 31: Max. contact pressure drop over time (3600 s)

3 Summary

A thermo-rheological material model was created based on a dynamic thermal analysis coupled with a hyperelastic model. the exposition of an EPDM O-ring to a load sequence up to p = 1000 bar and down to T = -50°C was simulated. The results showed a low tendency to gap extrusion and stresses in the groove of about 320 MPa. Furthermore, the contact pressure was evaluated. The sealing effect is sufficient for the applied system pressure in all conditions.

In addition, an estimate of the contact pressure reduction due to relaxation was calculated. This estimation gives a reduction of approximatively 5.5% at p = 600 bar, T = 20°C after one hour of relaxation and approximatively of 9.4% after one day. This confirmed that the O-ring seal currently in use meets the application requirements.

4 Nomenclature

Variable	***Description***	***Unit***
A_{EU}	Activation energy - lower range	[kJ/mol]
A_{EO}	Activation energy - upper range	[kJ/mol]
E'	Storage Modulus	[MPa]
E''	Loss Modulus	[MPa]
E^*	Complex Modulus	[MPa]
E_0	Glass Modulus	[MPa]
E_∞	Relaxations Modulus	[MPa]
$\tan\delta$	Tangent of loss angle	[-]
a_{T}	Shift-factor - temperature	[-]
C	Temperature - pressure shift ratio	[K/bar]
a_{p}	Shift-factor – pressure	[-]
e_{i}	Relaxation strength	[-]
τ_{i}	Relaxation time	[s]
$\sigma_{\mathrm{un}}, \sigma_{bi}$	Engineer stress (uniaxial, biaxial)	[MPa]
λ	Elongation (stretching)	[-]
c_{10}, c_{01}	Parameters for Mooney-Rivlin model	[MPa]
f	Frequency	[1/s], [Hz]
p	Pressure (1 bar = 10^5Pa = 0.1 MPa)	[bar], [MPa]
R	Molar gas constant	[kJ/mol K]
T	Temperature	[°C], [K]
T_{g}	Glass transition temperature	[°C], [K]
T_{ref}	Reference temperature	[°C], [K]
M	Conversion from ln to lg, $(M = lg(e) = 0.4343)$	[-]
N	Number of Prony parameters	[-]

5 References

[1] Herdy, M.: *Introductory Theory Manual ViscoData & ViscoShift, Version_0.53,* http://www.viscodata.de/Short_Introduction.pdf , visited 1 June 2022

[2] Ferry, J.D.: Viscoelastic properties of polymers. Third Edition, 1980, John Wiley & Sons, Inc. ISBN 0-471-04894-1

[3] Fillers, R., Tschoegl, N.W.: *The Effect of Pressure on the Mechanical Properties of Polymers. Transactions of the Society of Rheology 21, 51 (1977);* https://doi.org/10.1122/1.549463

[4] Bergström, J.: *Mechanics of Solid Polymers, © 2015 Elsevier Inc.* http://dx.doi.org/10.1016/B978-0-323-31150-2.00001-7

6 Authors

Eugen Seitz AG,

Spitalstrasse 204, 8623 Wetzikon, Switzerland:

Agim Gashi, Dipl.-Ing. FH, agashi@seitz.ch

Lucian Pasieka, Dr. rer. nat., Dipl.-Ing., lpasieka@seitz.ch

Eugen Seitz AG

Address:

Spitalstrasse 204, 8623 Wetzikon, Switzerland